A method to separate temperature and precipitation signals encoded in tree-ring widths for the western Tien Shan Mountains, northwest China

Wenhuo Liu[a, b], Xiaohua Gou[a*], Jinbao Li[c], Yuxia Huo[a] , Keyan Fang[d]

[a] Key Laboratory of Western China′s Environmental Systems (MOE), College of Earth and Environmental Sciences, Lanzhou University, Lanzhou 73000, China

[b] Department of Earth Sciences, University of Southern California, Los Angeles, California 90089, USA

[c] Department of Geography, University of Hong Kong, Hong Kong, China

[d] Key Laboratory of Humid Subtropical Eco-geographical Process (MOE), College of Geographical Sciences, Fujian Normal University, Fuzhou 350007, China.

*** Corresponding authors**

tel. +86 931 8915309

fax +86 931 8912330

e-mail: xhgou@lzu.edu.cn (X. Gou)

Abstract:

Separating temperature and precipitation signals encoded in tree rings is a complicated issue. Here, we present a separation method by combining two tree-ring width chronologies of Schrenk's spruce (*Picea schrenkiana*) from the upper and lower timberlines in the western Tien Shan Mountains, northwest China. Correlation analyses show that both chronologies correlate positively with precipitation. However, temperature correlates positively with the chronology from the upper timberline, while negatively with the chronology from the lower timberline. This suggests that the two chronologies contain similar precipitation information but opposite temperature signals. In light of this, we calculated the average and difference of the two chronologies, and found that each of them has a much stronger correlation with precipitation or temperature alone. Finally, we reconstructed local precipitation and temperature variations over the past 201 years by using the average and difference of the two chronologies. The two reconstructions do not have a significant correlation, but they have significant positive and negative relationships on the high- and low-frequency band, respectively.

Keywords: climate signals, tree rings, timberline, climate reconstruction, Tien Shan Mountains, dendroclimatology

1. Introduction

Temperature and precipitation are the two most important factors affecting tree growth, and are often recorded in tree-ring width chronologies simultaneously. However, the correlation patterns of the chronologies with temperature and precipitation are different at different altitudes. For example, previous studies from the arid and semiarid areas in northern China have shown that the chronologies from the middle to lower forest zones are generally positively correlated with precipitation, but negatively with temperature (Chen et al., 2015; Chen et al., 2012; Fang et al., 2010; Fang et al., 2012; Li et al., 2007; Li et al., 2006; Liang et al., 2006; Liu et al., 2009a; Shao et al., 2005; Sheppard et al., 2004; Song and Liu, 2011; Yang et al., 2011; Zhu et al., 2004). Although the chronologies from these altitudes are mainly used to study the precipitation variability (Chen et al., 2012; Liang et al., 2006; Liu et al., 2009a; Shao et al., 2005; Sheppard et al., 2004; Yang et al., 2011), more and more chronologies are found to have stronger relationships with the Palmer Drought Severity Index (PDSI) (Chen et al., 2015; Fang et al., 2010; Fang et al., 2012; Li et al., 2007; Li et al., 2006; Song and Liu, 2011; Tian et al., 2007). The PDSI is a direct metric of moisture conditions taking both temperature and precipitation into account (Dai et al., 2004; Palmer, 1965). This suggests that temperature also has an important influence on tree growth in the middle to lower forest zones. By contrast, the chronologies from the upper timberline are generally correlated positively with both temperature and precipitation (Liu et al., 2005; Liu et al., 2009b; Liu et al., 2006; Yu et al., 2007; Zhang et al., 2014; Zhu et al., 2004; Zhu et al., 2008). These chronologies were mainly used to study the temperature variability (Liu et al., 2005; Liu et al., 2009b; Yu et al., 2007; Zhang et al., 2014; Zhu et al., 2008). But some of them were also used to reconstruct precipitation (Liu et al., 2006), suggesting that precipitation also plays an important role on tree growth in the upper timberline. Obviously, we should separate the two climate signals encoded in tree rings in order to get more reliable precipitation and temperature reconstructions.

To our knowledge, there is no valid method to separate temperature and precipitation signals recorded in tree-ring width chronologies yet. The aforementioned studies showed that the chronologies from the middle to lower forest zones and the upper timberline are both positively correlated with precipitation, but have opposite relationships with temperature. Moreover, most of the chronologies showed similar response to temperature and precipitation in the same season (Chen et al., 2015; Chen et al., 2012; Fang et al., 2010; Fang et al., 2012; Li et al., 2007; Li et al., 2006; Liang et al., 2006; Liu et al., 2009a; Shao et al., 2005; Sheppard et al., 2004; Song and Liu, 2011; Tian et al., 2007; Yang et al., 2011; Yu et al., 2007; Zhang et al., 2014; Zhu et al., 2004). In view of this, here we propose to use the average and difference of the chronologies from the middle to lower forest zones and the upper timberline to separate the precipitation and temperature signals, so as to extract purer precipitation and temperature information.

In this paper, we present two chronologies from the lower and upper timberlines in the western Tien Shan Mountains, northwest China. As shown below, the climate responses of the two chronologies are similar to that of the above studies. Therefore, we combine them to identify whether the precipitation and temperature signals in the chronologies can be separated by statistical means.

2. Materials and Methods

2.1. Tree-ring data

In China, the Tien Shan Mountains extend about 1,300 km from the Hami district of Xinjiang province in the east to the national boundaries of China and Kazakhstan in the west. The Tien Shan Mountains block the humid air that is transported from the Atlantic and Arctic oceans under the influence of the westerlies, leading to more precipitation in the northern slope of the Tien Shan Mountains and a gradual decrease of rainfall from west to east. This is also the main factor responsible for the growth of coniferous forests on the northern slope of the Tien Shan Mountains. Generally, coniferous forests occur on shady and semi-shady slopes at 1,400–2,800 m a.s.l. The forest vegetation is primarily composed of *Picea schrenkiana*, while a mix of *P. schrenkiana* and *Larix sibirica* forests are present in the easternmost Tien Shan Mountains.

Tree-ring samples were collected from two sites, KUE and WUY, in the western Tien Shan Mountains (Fig. 1, Table 1). KUE is located at the lower timberline with an average elevation of 1499 m a.s.l. WUY is near to the upper timberline with an average elevation of 2763 m a.s.l. Increment cores were taken from *P. schrenkiana* at both sites. For cross-dating, at least 20 dominant trees were selected and two cores per tree were taken at breast height using 5-mm increment borers. In total, 46 (44) cores from 23 (23) trees were retrieved at the site of KUE (WUY), respectively.

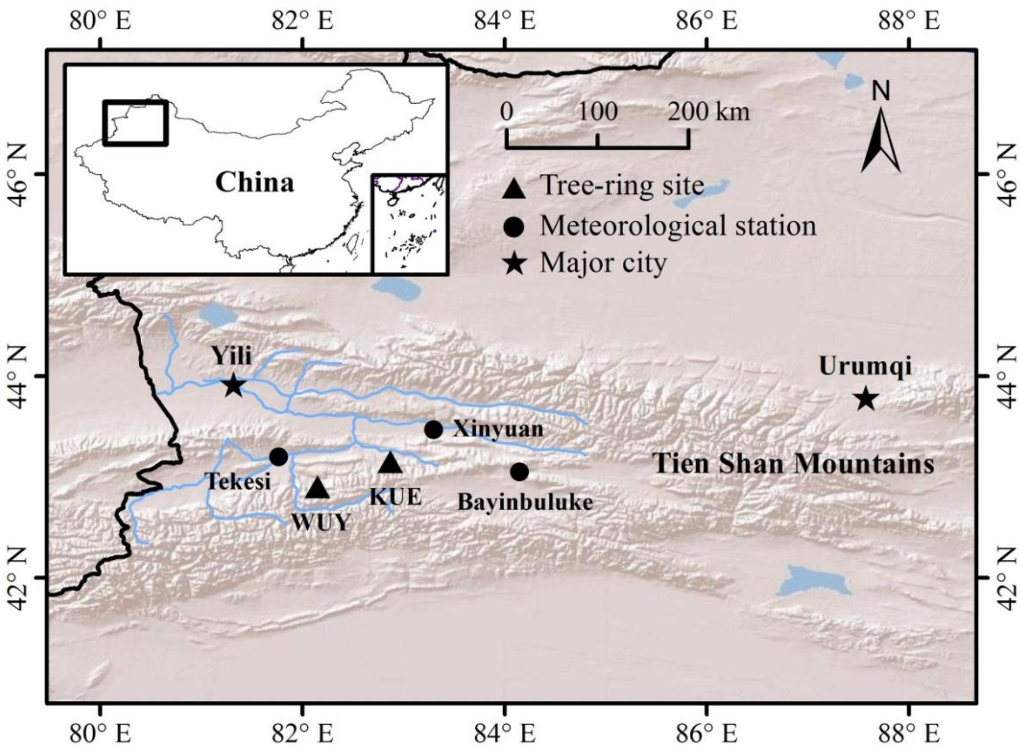

Fig. 1 Locations of tree-ring sampling sites (KUE and WUY) and the nearby meteorological stations (Tekesi, Xinyuan and Bayinbuluke).

Table 1 Statistics of the two tree-ring sampling sites and the nearby meteorological stations.

Data type	Site code	Location (Latitude, Longitude)	Elevation (m)	Samples (Core/Tree)	Time span (AD)
Tree-ring data	KUE	43°09′16.1″ N, 82°52′29.1″ E	1499	46/23	1634–2004
	WUY	42°53′11.9″ N, 82°08′34.5″ E	2763	44/23	1690–2004
Meteorological data	Tekesi	43°11′N, 81°46′E	1211	–	1960–2004
	Xinyuan	43°27′N, 83°18′E	929	–	1956–2004
	Bayinbuluke	43°02′N, 84°09′E	2458	–	1958–2004

In the laboratory, standard dendrochronological techniques were used to process the tree-ring cores. After air drying, mounting and sanding, all the samples were carefully cross-dated by visual comparison, and each ring-width was subsequently measured to 0.001 mm precision. The COFECHA program (Holmes, 1983) was further employed to check the quality of visual cross-dating. These methods ensure exact dating for each annual growth ring.

The chronologies were developed with the ARSTAN program (Cook, 1985) by removing biological growth trends while preserving variations that were likely related to climate. In most cases, we adopted negative exponential functions or linear functions to detrend the tree-ring series (83 series). A few of the series (7 series), which did not fit the negative exponential or linear models, were detrended by the cubic spline models. The detrended series were finally processed to produce the mean chronology using a bi-weight mean method. The variations of the two chronologies are shown in Fig. 2. Because the sample size declined in the early portion of the tree-ring chronology, the subsample signal strength (SSS) value of 0.85 (Wigley et al., 1984) was suggested to determine the reliable period of the chronology. In this study, the reliable period of the chronology with SSS values above 0.90 was used for further analyses. The final KUE and WUY chronologies extend from 1764–2004 AD and 1804–2004 AD, respectively.

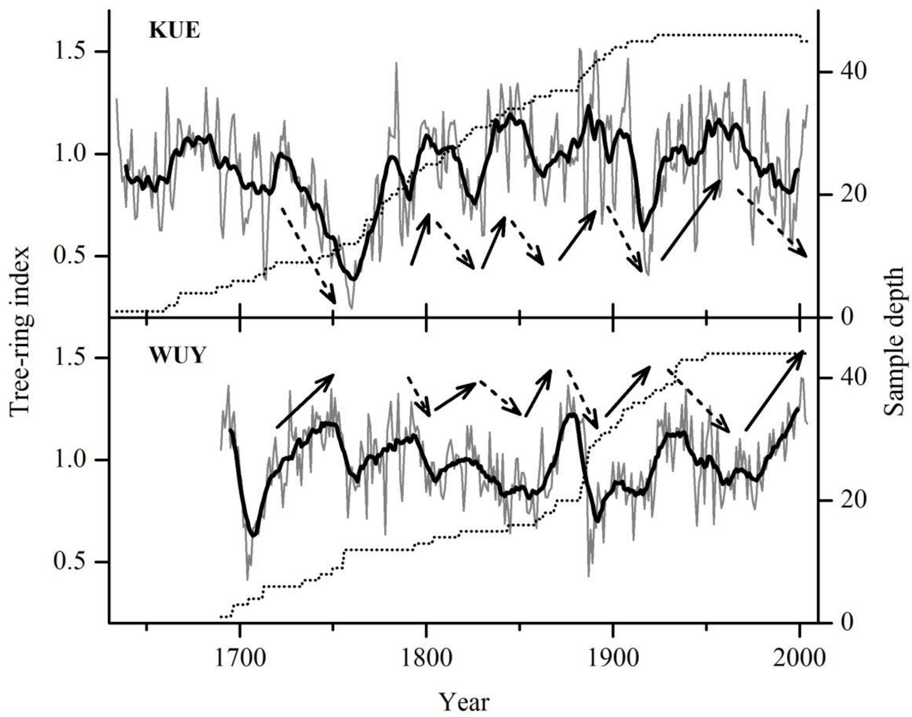

Fig. 2 Standardized tree-ring width chronologies (solid line) and corresponding sample depth (dot line). The bold line indicates an 11-year running mean. The solid and dash arrows indicate the rising and decreasing parts of the tree-ring indices, respectively.

2.2. Data analysis

Monthly mean temperature and precipitation records were obtained from three nearby meteorological stations, i.e. Tekesi, Xinyuan and Bayinbuluke (Fig. 1 & Table 1). Tekesi and Xinyuan are nearest to WUY and KUE, respectively. Tekesi and Bayinbuluke have the most similar elevations to KUE and WUY, respectively. As both sampling sites are located in the middle of the three meteorological stations, the mean values of climate variables from the three stations were calculated to better represent climate variations at the sample sites and to investigate the climate–tree growth relationships.

Fig. 3 shows the monthly distributions of regional temperature and precipitation. It can be seen that high temperatures are generally associated with high precipitation, and vice versa. January and July are the coldest and warmest months, and February and June are the driest and wettest months, respectively. The annual total precipitation is 384.2mm, 76.8% of which falls in April–September, when the monthly mean temperatures are all above 5 ℃. It is clear that April–September can be considered as the growing season in the study area.

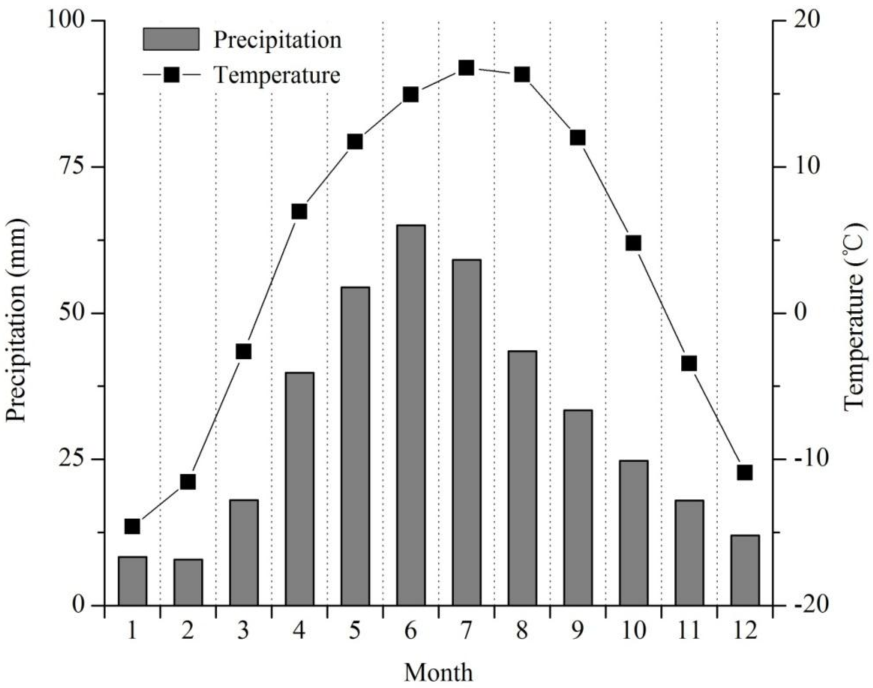

Fig. 3 Monthly distribution of temperature and precipitation of the study area during 1960–2004. Temperature and precipitation values were calculated by taking the numerical mean of all three meteorological stations.

3. Results and discussion

3.1. Characteristics of the chronologies

Table 2 shows the statistical characteristics of the two chronologies, including mean sensitivity (MS), first-order autocorrelation (AC1), mean correlations among all radii (R1), mean correlations between trees (R2), mean correlations within trees (R3), Signal-to-noise ratio (S/N), Expressed Population Signal (EPS) and the explained variance by the first eigenvector (PC1). The chronologies with higher MS and AC1 mean that they contain more high- and low-frequency information, respectively. The sites with larger R1, R2, R3, S/N, EPS and PC1 mean that their tree-ring series were more consistent with each other. As shown in Table 2, the statistical characteristics of KUE are all higher than that of WUY. Similar patterns are also found in other semi-arid regions in the northwest China (e.g., Gou et al., 2005; Peng et al., 2006; Peng et al., 2008; Wang et al., 2005; Zhu et al., 2004).

Table 2 Statistical characteristics of the two standardized tree-ring chronologies

Statistical item	KUE	WUY
Mean Sensitivity (MS)	0.153	0.129
First-order autocorrelation (AC1)	0.724	0.649
Common period	1900–1999	1900–1999
Mean correlations among all radii (R1)	0.336	0.252
Mean correlations between trees (R2)	0.338	0.244
Mean correlations within trees (R3)	0.714	0.581
Signal-to-noise ratio (S/N)	22.296	10.776
Expressed Population Signal (EPS)	0.957	0.915
Variance explained by the first eigenvector (PC1)	38.6%	28.9%
Subsample Signal Strength (SSS)>0.90	1764–2004	1804–2004

Although the two sampling sites are close to each other, the correlation between the chronologies is almost zero (r=0.026) during the common reliable period 1804–2004 AD. This is at least partially due to the large difference in their elevations (Table 1). It should be noted that the two chronologies have a significant positive relationship (r=0.173, n=249, p<0.01) after 10-year high-pass filtering. However, there was a negative relationship (r=–0.262) after smoothing with an 11-year moving average. As shown in Fig. 2, the growth trends of the two chronologies were opposite in many intervals during the common period. This may suggest that the two chronologies contain similar information in their high-frequency band, but have opposite signals in their low-frequency band. This may be the reason why overall the two chronologies were not significantly correlated with each other.

3.2. Climate signals in tree-ring widths

The Pearson correlations of the two chronologies with monthly temperature and precipitation data from previous May to current October during the common period 1960–2004 are shown in Fig. 4. It can be seen that the two chronologies are, in general, positively correlated with precipitation, suggesting that precipitation is a key limiting factor on tree growth in the study area, not only at the lower timberline but also at the upper timberline. This phenomenon is also found in many other tree-ring studies in arid and semiarid areas of northwest China (Chen et al., 2015; Gou et al., 2005; Liang et al., 2006; Liu et al., 2009a; Liu et al., 2005; Liu et al., 2006; Shao et al., 2005; Wang et al., 2005; Yang et al., 2011; Zhu et al., 2004). The highest correlations of the KUE and WUY chronologies with seasonal precipitation were found in July–April (from prior July to current April) ($r=0.495$, $p<0.01$, $n=44$) and August–July ($r=0.577$, $p<0.01$, $n=44$), respectively. The correlation of the WUY chronology with the July–April precipitation was 0.545, which is only a little lower than 0.577. This suggests that the two chronologies recorded similar seasonal precipitation information.

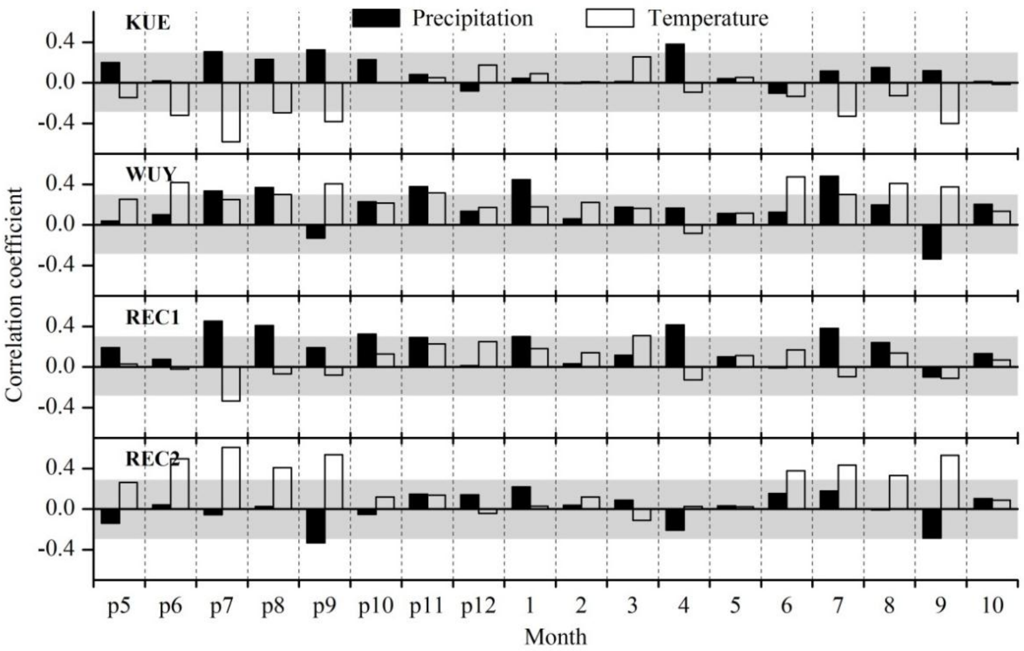

Fig. 4 Correlations of tree rings with monthly temperature and precipitation records during the common period 1960–2004. REC1 and REC2 are the average and difference of the WUY and KUE chronologies, respectively. p means the prior year; all bars that exit the shaded area indicate significance at $p<0.05$.

Unlike precipitation, monthly temperatures were generally negatively correlated with the KUE chronology, but positively with the WUY chronology. High correlations are generally found in the growing seasons of the previous and current years (Fig. 4), suggesting that both chronologies record temperature signals in the same season, but with opposite signs. Such opposite growth–temperature relationships between the lower and upper timberlines are also found in many other tree-ring studies in arid and semiarid areas in northwest China (Chen et al., 2015; Liu et al., 2009a; Liu et al., 2005; Peng et al., 2008; Yang et al., 2011; Zhang et al., 2014; Zhu et al., 2004). This may be one of the reasons why there were opposite relationships between low-frequency variations of the two chronologies (Fig. 2). The opposite relationships suggest different influences of temperature on tree growth at the lower and upper timberlines. At the upper timberline, temperature is very low and thus limits tree growth. In contrast, at the lower timberline, temperature is high and thus limits tree growth. High temperature also leads to high evaporation, and thus may indirectly affect tree growth in arid and semiarid areas.

Because the two chronologies have similar precipitation signals and opposite temperature signals, we calculated their average (REC1) to identify whether their temperature signals could be offset with each other. As shown in Fig 4, the correlations between REC1 and the monthly temperatures were generally very low, especially in the growing seasons of the previous and current years when both of the KUE and WUY chronologies had high correlations with the temperatures. The highest correlation between REC1 and the seasonal temperature occurred in November–March, which was only 0.365, suggesting that there is little temperature information recorded in REC1. In contrast, the correlations of REC1 with the monthly precipitation were very high. The highest correlation between REC1 and seasonal precipitation occurred in July–April, with a correlation up to 0.739. Obviously, we got a purer and stronger precipitation signal after calculating the average of the two chronologies.

We also calculated the correlations between the difference of the two chronologies (i.e. WUY minus KUE) (REC2) and the monthly climate data. As shown in Fig. 4, the correlations between REC2 and the monthly precipitation were generally very low, except for September of the previous and current years, while the correlations between REC2 and the monthly temperatures were still very high and even were improved during the growing seasons of the previous and current years. Further analysis showed that there were no significant correlations between REC2 and the seasonal precipitation, while the highest correlation between REC2 and seasonal temperatures was up to 0.741, which occurred in June–September of the prior year. These results suggest that REC2 mainly recorded the temperature signals.

The highest correlations of REC1 with July–April precipitation and REC2 with previous June–September temperature suggested that both precipitation and temperature in the previous growing season played very important roles in modulating tree growth in the study area. It was probably because that the better precipitation and temperature conditions during the previous growing season might enhance photosynthesis rates, which could lead to higher carbohydrate storage, and thus to increase growth in the following year (Fritts, 1976). The significant effect of climate in the previous growing season on tree growth could also be found in many other tree-ring studies in arid and semiarid areas across northern China (Chen et al., 2010; Chen et al., 2012; Gou et al., 2008; Liang et al., 2006; Liu et al., 2009a; Shao et al., 2005; Sheppard et al., 2004; Shi et al., 2010; Tian et al., 2007; Wang et al., 2005; Yang et al., 2011; Yu et al., 2008; Yuan et al., 2001). This suggests that the close relationships of tree-ring widths in the study area with climate of the previous growing season have a physiological meaning.

3.3. Precipitation reconstruction

The above analyses demonstrated that the REC1 contained almost no temperature information, but its correlation with July–April precipitation was strong enough for reconstruction. Considering that the weight of the precipitation and temperature signals may be different and that the two chronologies were uncorrelated and did not have the same amplitude of variation, we used the KUE and WUY chronologies as predictors to reconstruct the precipitation using a multiple linear regression model. The model is as follows:

$$P_t = 110.308 \times KUE_t + 174.814 \times WUY_t - 23.975 \quad \ldots\ldots\ldots\ldots(1)$$

where P_t is the total precipitation from prior July to current April in t year, and KUE_t and WUY_t are the tree-ring width indices of the KUE and WUY chronologies in t year, respectively. During the calibration period 1960–2004, the reconstructed series explained 57.8% (55.8% after degree of freedom is adjusted) of the observed precipitation. As shown in Fig. 5a, the reconstruction successfully captured both high-and low-frequency variations of the observed precipitation.

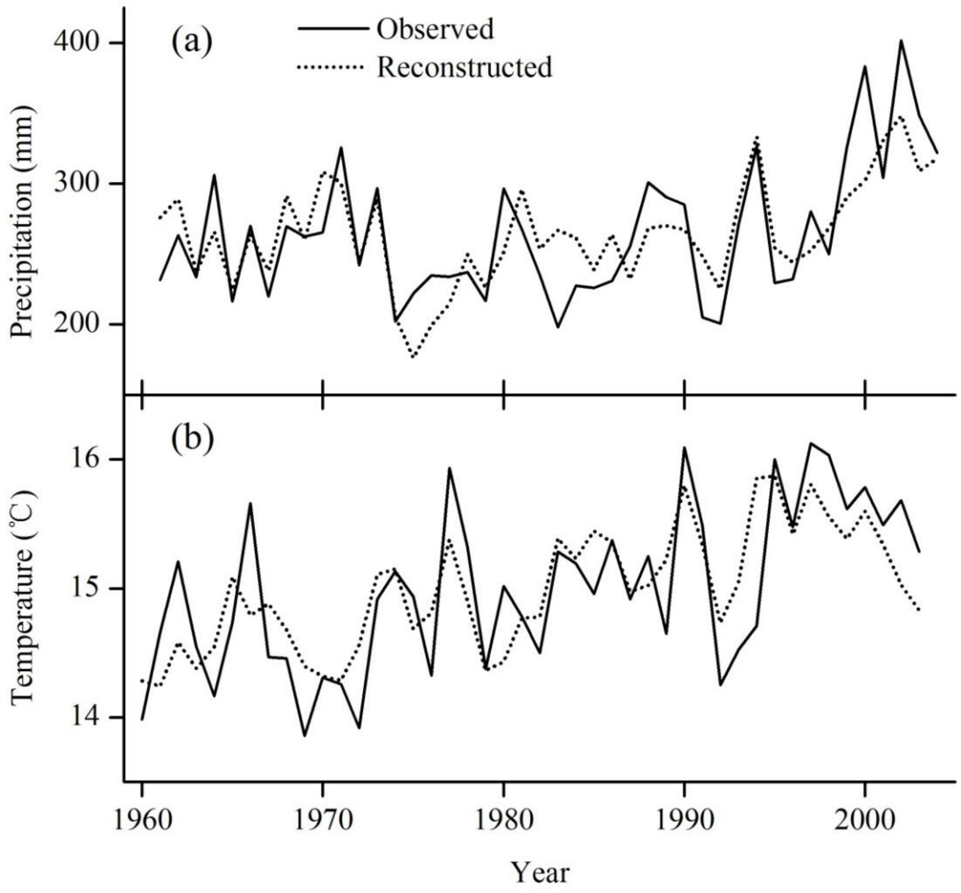

Fig. 5 Comparison of the observed and reconstructed (a) precipitation and (b) temperature during the calibration periods.

Since there are only 45 years (1960–2004) of the observed meteorological data, we used the leave-one-out test (Mosteller and Tukey, 1977) to explore the stability of the model. The resulting statistics are shown in Table 3. It can be seen that the values of r, F-statistics (F), sign test (S1), 1st-difference sign test (S2) and product means test (t) are all above the 0.05 significance level, indicating that the predicted values agree closely with the actual data. In addition, the value of the reduction of error (RE) test is greater than zero, indicating rigorous model skill (Cook et al., 1999). Therefore, we used the model (1) to reconstruct the July–April precipitation in the study area.

Table 3 Calibration and verification test for the period 1960–2004.

Model	r	R^2	$R^2_{aj.}$	F	S1	S2	t	RE
(1)	0.760**	0.578	0.558	28.095**	35+/9–**	30+/13–*	4.331**	0.519
(2)	0.744**	0.554	0.532	25.485**	33+/11–**	29+/14–*	4.317**	0.509

Note: r, correlation between observed and estimated series; R^2, explained variance; $R^2_{aj.}$, explained variance after degree of freedom is adjusted; F, F-statistics; the sign test counts the agreements and disagreements (S1, S2) between the observed and estimated departures from the mean; S1 is the general sign test between observation and reconstruction that measures the association at all frequencies; S2 is a similar test, but made for the first differences thus reflecting the high-frequency climatic variation; t, product mean; RE, reduction of error; ** and * indicate significance at the 0.01 and 0.05 levels, respectively.

Fig. 6a shows the annual precipitation reconstruction over the past 201 years (1804–2004 AD), and its 11-year running mean. The mean value of the reconstructed precipitation over the whole period is 254.8 mm with a standard deviation (σ) of 40.6 mm. We defined the dry years as those that were less than mean−1σ (214.2 mm) and the wet years as those that were greater than mean+1σ (295.4 mm). The dry years and the wet years accounted for 16.9% (34 years) and 15.9% (32 years) of the entire reconstruction period, respectively. Fortunately, most of the dry years and the wet years lasted less than 2 years. The dry periods that persisted over 2 years were found in 1829–1831, 1914–1919 and 1974–1976, and the wet periods that persisted over 2 years occurred in 1882–1884, 1950–1953 and 2000–2004.

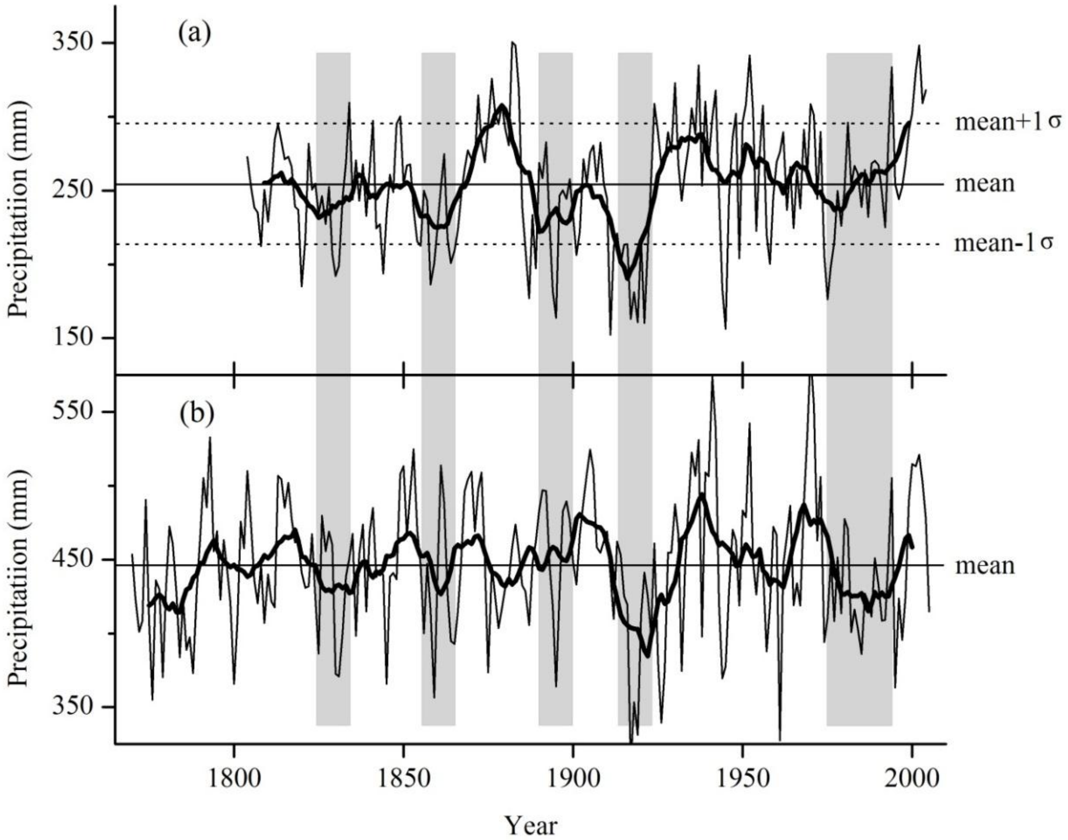

Fig. 6 Comparison of the precipitation reconstructions developed by (a) this study, and (b) Chen et al (2010). Thick line indicates an 11-year running mean. σ means the standard deviation of the annual precipitation reconstruction.

In order to understand whether our precipitation reconstruction is reliable, we compared it with a July–June precipitation reconstruction in the study area, which was developed by a traditional method (i.e. using the chronologies which have high correlations with precipitation but have low correlations with temperatures to conduct precipitation reconstructions) (Chen et al., 2010). As shown in Fig. 6, the two precipitation reconstructions were quite consistent with each other over the common period 1804–2004 AD, with a correlation of 0.549 ($p<0.01$). This suggests that our reconstructed method is useful, and the precipitation reconstruction is reliable.

The multi-taper method (MTM) of spectral analysis (Mann and Lees, 1996) was employed to examine the characteristics of the precipitation reconstruction in the frequency domain. As shown in Fig. 7a, the significant cycles above the 0.05 level were found at 2.0–2.3 and 5.1–5.5 years, particularly significant at 2.0 years ($p<0.01$). These cycles resemble those reported in other findings in surrounding areas (Chen *et al.*, 2010). All of these cycles not only fall within the range of El Niño-Southern Oscillation (ENSO) variability (Allan et al., 1996; Li et al., 2013), but also are within the signal bands of the Arctic Oscillation (AO) (Jevrejeva, 2003). The strong biennial cycle (2.0–2.1 years) also resembles the variability of tropical biennial oscillation (TBO; Meehl, 1987). Overall, these cycles suggest that precipitation variability in the study area may have strong associations with large-scale ocean–atmosphere–land circulation systems.

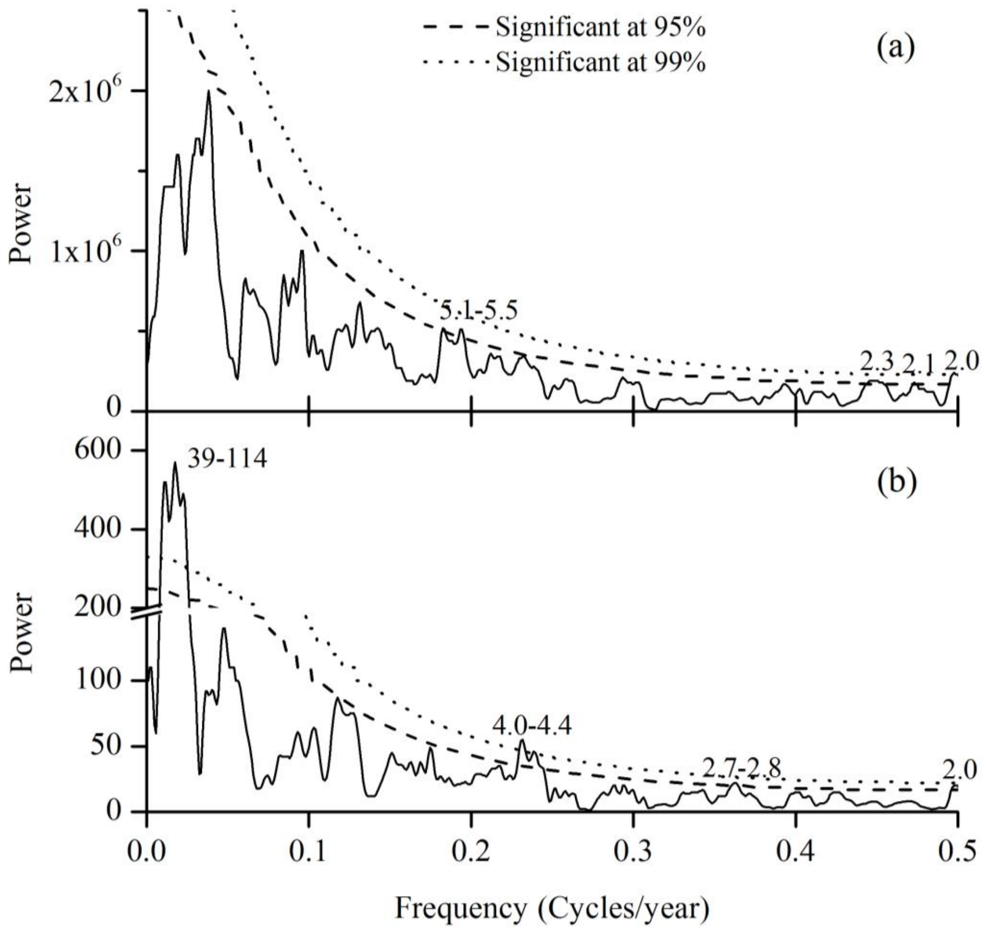

Fig. 7 MTM spectral density of the (a) precipitation and (b) temperature reconstructions. The dash and dotted lines indicate the 95 and 99% significance levels, respectively.

3.4. Temperature reconstruction

Similar to our precipitation reconstruction, we used the two chronologies as predictors to reconstruct the temperature variability. Because the highest correlation of REC2 with the seasonal temperatures occurred in previous June–September, the following temperature reconstruction only focused on this season. The equation is as follows:

$$T_t = -1.499 \times KUE_{t+1} + 1.827 \times WUY_{t+1} + 14.535 \ldots\ldots\ldots\ldots (2)$$

where T_t is the mean temperature from June to September in t year, and KUE_{t+1} and WUY_{t+1} are tree-ring width indices of the KUE and WUY chronologies in t+1 year, respectively. During the calibration period of 1960–2004, the reconstruction captured 55.4% (53.2% after the degree of freedom is adjusted) of the observed temperature variance. As shown in Fig. 5b, our reconstruction successfully captured both high- and low-frequency variations of the observed temperature.

We also used the leave-one-out test (Mosteller and Tukey, 1977) to explore the stability of the model (2). The resulting statistics (Table 3) indicate the validity of our regression model. Therefore, we used the model (2) to reconstruct the June–September temperature in the research area.

Fig. 8a shows the annual June–September temperature reconstruction over the past 201 years (1803–2003 AD) and its 11-year running mean. It can be seen that the temperature reconstruction contains considerable low-frequency variability. If the mean (14.8°C) of the temperature reconstruction over the whole period was considered as a reference, the cold periods occurred during the 1803–1810s, 1830s–1860s, 1880s–1900s and 1950s–1970s, and the warm intervals were found during the 1820s, 1870s, 1910s–1940s and 1980s–2004. Of these, the 1887–1896 and 1994–2003 periods were the coldest and warmest 10 years, respectively.

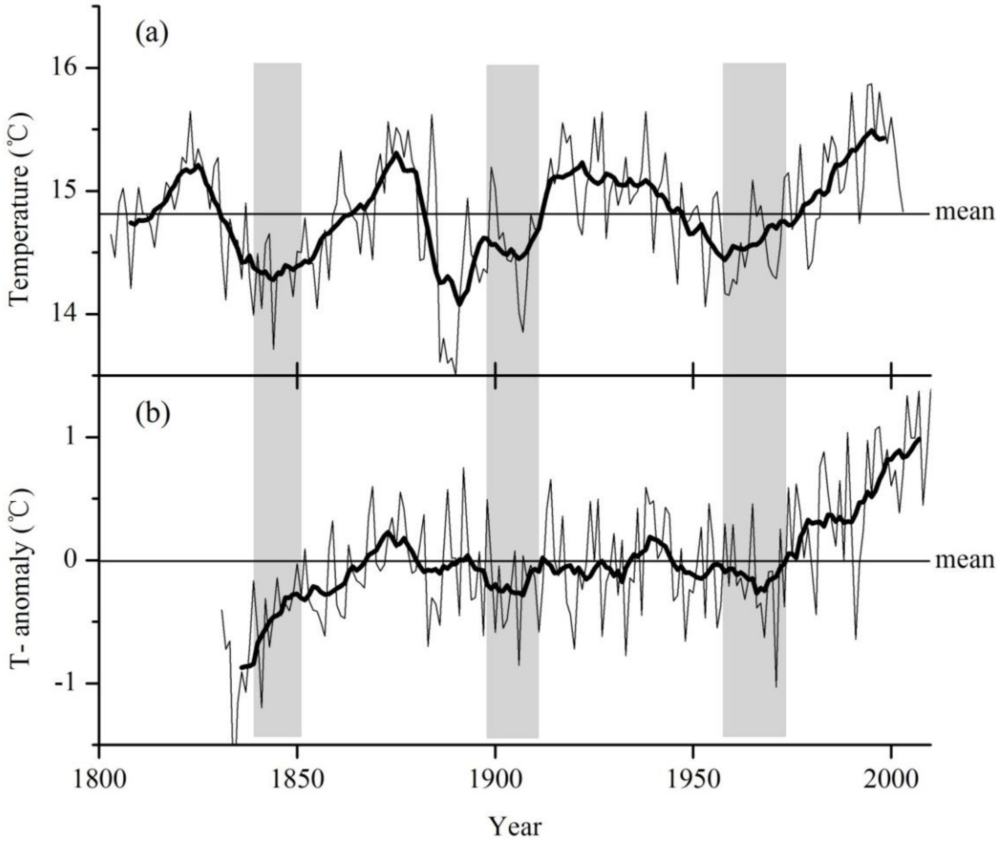

Fig. 8 Comparison of (a) the temperature reconstruction developed by this paper, and (b) the regional (35°N–45°N, 65°E–90°E) average temperature in June–September derived from the Berkeley Earth gridded temperature anomaly dataset (Rohde et al., 2013). Thick line indicates an 11-year running mean.

In order to understand whether our temperature reconstruction is reliable, we compared it with a regional (35°N–45°N, 65°E–90°E) average temperature in June–September, which is derived from the monthly gridded temperature anomaly dataset developed by Berkeley Earth (Rohde et al., 2013). As shown in Fig. 8, our reconstruction agrees well with this regional temperature over the common period of 1832–2003 AD, and their correlations are 0.451 ($p<0.01$, $n=172$) and 0.697 in the annual and 11-year average variability, respectively. It should be noted that there was less consistency during the early time. This may be due to the less reliable regional temperature record due to the sparse observational data in the early part of the period. Overall, our reconstruction performed well in reproducing the temperature history of the study area.

The results of the multi-taper method (MTM) of spectral analysis (Mann and Lees, 1996) over the full length of the temperature reconstruction revealed significant periods at 2.0, 2.7–2.8, 4.0–4.4, and 39–114 years (Fig. 7b). The significant high-frequency cycles may be also related to ENSO, AO, and TBO variations, and the 39–114 year cycle may be affected by the solar activity (Usoskin and Mursula, 2003). It should be noted that the cycles with longer 100 years may be less reliable, because they could not occur twice completely over the whole reconstruction period. Unlike the precipitation reconstruction, the most significant cycle of the temperature reconstruction is 39–114 years ($p<0.01$) (Fig. 7b), suggesting that the low-frequency variability of the temperature reconstruction is more prevalent than that of the precipitation reconstruction. This also can be confirmed from Fig. 6a and 8a. Compared with the early tree-ring width based temperature reconstructions in the western Tien Shan Mountains (Chen et al., 2009; Fan et al., 2008; Pan et al., 2007; Shang et al., 2011; Yu et al., 2007; Yu et al., 2008), our temperature reconstruction also has stronger low-frequency variability. This is at least partially due to the fact that the precipitation signals of the tree-ring chronologies have been eliminated in our temperature reconstruction. In addition, most of these early reconstructions focused on studying the seasonal maximum temperatures (Chen et al., 2009; Fan et al., 2008; Pan et al., 2007; Shang et al., 2011), which also showed more high-frequency variability in many other studies over the world (e.g., Arsalani et al., 2015; Etien et al., 2007; Gou et al., 2008; Shi et al., 2010; Wilson and Luckman, 2003). Moreover, some reconstructions were developed using the residual (RES) chronologies (Chen et al., 2009; Pan et al., 2007), which lack low-frequency variability.

3.5. Comparison of the precipitation and temperature reconstructions

To our knowledge, there have been no studies attempted to compare precipitation and temperature variations in the western Tien Shan Mountains over the past centuries, despite the fact that many tree-ring based precipitation and temperature reconstructions have been developed in the area (Chen et al., 2009; Chen et al., 2010; Fan et al., 2008; Pan et al., 2007; Shang et al., 2011; Yu et al., 2007; Yu et al., 2008; Yuan et al., 2001). This is at least partially due to the lack of a method to separate the temperature and precipitation signals recorded in tree rings. Because the precipitation and temperature signals have been separated, the use of our reconstructions to investigate the precipitation and temperature relationship in the western Tien Shan Mountains over the past centuries should be feasible.

There is a 3-month overlap (i.e. July to September) between the two reconstruction seasons. During the instrumental period, the seasonal precipitation in prior July–September had a high correlation with that in July–April ($r=0.746$), and the correlation of the seasonal temperature in July–September and June–September was up to 0.938, suggesting that our reconstructions can approximately represent the precipitation and temperature variability for the overlap months. Correlation analyses showed that overall the two reconstructions did not have any relationship, with a correlation near to zero (r=0.060). However, after removing the low-frequency variability (10-year high-pass filtering), the two series have a significant negative correlation ($r=-0.213$, $p<0.01$, $n=201$). In contrast, the two series have a positive correlation (r=0.291) after smoothing with an 11-year moving average. These correlation patterns are similar to that observed during the instrumental period (not shown). This suggests that the precipitation and temperature variations in the study area were similar in the low-frequency band, but were opposite in the high-frequency band, at least for the past two centuries.

4. Conclusions

We developed two tree-ring width chronologies from the upper and lower timberlines in the western Tien Shan Mountains, northwest China. Correlation analyses showed that the two chronologies have similar precipitation information but opposite temperature signals. In light of this, we calculated the average of the two chronologies, and found that the opposite temperature signals can be offset and the precipitation information can still be preserved and enhanced. On the other hand, the precipitation information can be eliminated and thus the temperature signals can be preserved and enhanced by calculating the difference between the two chronologies. As a result, the temperature and precipitation signals recorded in tree rings can be well separated with this method, which helps conduct a more reliable temperature and precipitation reconstruction. Finally, we successfully reconstructed regional July–April precipitation (1804–2004AD) and June–September temperature (1803–2003AD) using different combinations of the two chronologies. The temperature reconstruction contains considerable low-frequency variability during the past two centuries, with the most significant cycle at 39–114 years ($p<0.01$), while the precipitation reconstruction exhibits strong high-frequency variability, with the most significant cycle at 2.0 years ($p<0.01$). Compared with the earlier studies in the western Tien Shan Mountains, our temperature reconstruction has stronger low-frequency but weaker high-frequency variability. This is may be partially due to the fact that the precipitation signals of the tree-ring chronologies have been eliminated in our temperature reconstruction. The two reconstructions do not have a significant correlation, but they have negative (positive) relationships in the high (low) frequency band, respectively, a feature that is also observed with instrumental data. The method we proposed to separate temperature and precipitation signals works well in our research area. Future study should test its feasibility in other areas around the world.

Acknowledgments

We thank Feng Chen for providing the precipitation reconstruction data. The kind help of Mark Nishibayashi for improving the language was highly appreciated. This research is supported by the National Natural Science Foundation of China (No.

41475067, No. 41171039 and No. 41401047). Wenhuo Liu is also funded by the China Scholarship Council (No. 201206180111).

References

Allan, R., Lindesay, J. and Parker, D., 1996. El Niño Southern oscillation and climatic variability. Csiro Publishing, Collingwood, Australia.

Arsalani, M., Azizi, G. and Bräuning, A., 2015. Dendroclimatic reconstruction of May–June maximum temperatures in the central Zagros Mountains, western Iran. Int. J. Climatol. 35(3), 408–416.

Chen, F. et al., 2015. Tree-ring recorded hydroclimatic change in Tienshan mountains during the past 500 years. Quat. Int. 358, 35–41.

Chen, F. et al., 2009. Spring mean maximum temperature series and its variation properties in Hutubi River Basin during the last 313 years. J. Desert Res. 29(1), 162–167 (in Chinese with English abstract).

Chen, F. et al., 2010. Variation and prediction trend of precipitation series for the Tekes River basin during the last 236 years. J. Mountain Sci. 28, 545–551 (in Chinese with English abstract).

Chen, Z. et al., 2012. Tree-ring based precipitation reconstruction for the forest–steppe ecotone in northern Inner Mongolia, China and its linkages to the Pacific Ocean variability. Global Planet. Change 86–87, 45–56.

Cook, E.R., 1985. A time series analysis approach to tree ring standardization. Dissertation for the Doctoral Degree. Tucson: University of Arizona.

Cook, E.R., Meko, D.M., Stahle, D.W. and Cleaveland, M.K., 1999. Drought reconstructions for the continental United States. J. Clim. 12(4), 1145–1162.

Dai, A., Trenberth, K.E. and Qian, T., 2004. A global dataset of Palmer Drought Severity Index for 1870–2002: relationship with soil moisture and effects of surface warming. J. Hydrometeorol. 5(6), 1117–1130.

Etien, N. et al., 2007. Maximum growing season temperature in Western Europe: multi proxy reconstructions in Fontainebleau from 1596 to 2000. Clim. Past Discuss. 3(5), 1063–1117.

Fan, M., Yuan, Y., Wei, W. and Yu, S., 2008. Interpolation and analysis of mean summer maximum temperature in Yili prefecture in the west Tianshan Mountains, China. Arid Zone Res. 25(1), 75–81 (in Chinese with English abstract).

Fang, K., Gou, X., Chen, F., D'Arrigo, R. and Li, J., 2010. Tree-ring based drought reconstruction for the Guiqing Mountain (China): linkages to the Indian and Pacific Oceans. Int. J. Climatol. 30(8), 1137–1145.

Fang, K. et al., 2012. Tree-ring based reconstruction of drought variability (1615–2009) in the Kongtong Mountain area, northern China. Global Planet. Change 80–81, 190–197.

Fritts, H.C., 1976. Tree rings and climate. London, New York, San Francisco.: Academic Press.

Gou, X. et al., 2008. Asymmetric variability between maximum and minimum temperatures in Northeastern Tibetan Plateau: Evidence from tree rings. Sci. China Ser. D-Earth Sci. 51(1), 41–55.

Gou, X. et al., 2005. Climatic response of thick leaf spruce (*Picea crassifolia*) tree-ring width at different elevations over Qilian Mountains, northwestern China. J. Arid Environ. 61(4),

513–524.
Holmes, R.L., 1983. Computer-assisted quality control in tree-ring dating and measurement. Tree-Ring Bull. 43, 69–78.
Jevrejeva, S., 2003. Influence of the Arctic Oscillation and El Niño-Southern Oscillation (ENSO) on ice conditions in the Baltic Sea: The wavelet approach. J. Geophy. Res. 108(D21), 4677, doi:10.1029/2003JD003417.
Li, J., Chen, F., Cook, E.R., Gou, X. and Zhang, Y., 2007. Drought reconstruction for North Central China from tree rings: the value of the Palmer drought severity index. Int. J. Climatol. 27(7), 903–909.
Li, J., Gou, X., Cook, E.R. and Chen, F., 2006. Tree-ring based drought reconstruction for the central Tien Shan area in northwest China. Geophy. Res. Let. 33, L07715, doi:10.1029/2006GL025803.
Li, J. et al., 2013. El Niño modulations over the past seven centuries. Nat. Clim. Change 3(9), 822–826.
Liang, E. et al., 2006. The 1920s drought recorded by tree rings and historical documents in the semi-arid and arid areas of northern China. Clim. Change 79(3–4), 403–432.
Liu, W. et al., 2009a. Drought reconstruction in the Qilian Mountains over the last two centuries and its implications for large-scale moisture patterns. Adv. Atmos. Sci. 26(4), 621–629.
Liu, X., Qin, D., Shao, X., Chen, T. and Ren, J., 2005. Temperature variations recovered from tree-rings in the middle Qilian Mountain over the last millennium. Sci. China Ser. D-Earth Sci. 48(4), 521–529.
Liu, Y. et al., 2009b. Annual temperatures during the last 2485 years in the mid-eastern Tibetan Plateau inferred from tree rings. Sci. China Ser. D-Earth Sci. 52(3), 348–359.
Liu, Y. et al., 2006. Precipitation variation in the northeastern Tibetan Plateau recorded by the tree rings since 850 AD and its relevance to the Northern Hemisphere temperature. Sci. China Ser. D-Earth Sci. 49(4), 408–420.
Mann, M.E. and Lees, J.M., 1996. Robust estimation of background noise and signal detection in climatic time series. Clim. Change 33(3), 409–445.
Meehl, G.A., 1987. The annual cycle and interannual variability in the tropical Pacific and Indian Ocean regions. Mon. Weather Rev. 115(1), 27–50.
Mosteller, F. and Tukey, J.W., 1977. Data analysis and regression. A second course in statistics. Addison-Wesley Series in Behavioral Science: Quantitative Methods, Reading, Mass.: Addison-Wesley.
Palmer, W.C., 1965. Meteorological drought. US Department of Commerce, Weather Bureau Washington, DC, USA.
Pan, Y., Yuan, Y. and Yu, S., 2007. Reconstruction and analysis of summer temperature sequence for Boertala River Basin over past 461 year. J. Desert Res. 27(1), 59–164 (in Chinese with English abstract).
Peng, J. et al., 2006. The responses of growth ring width variations of *Larix sibirica Ledb* to climatic change in eastern Tianshan Mountains. Acta Ecol. Sin. 26(8), 2723–2731 (in Chinese with English abstract).
Peng, J. et al., 2008. Altitudinal variability of climate–tree growth relationships along a consistent slope of Anyemaqen Mountains, northeastern Tibetan Plateau. Dendrochronologia 26(2), 87–96.
Rohde, R. et al., 2013. A new estimate of the average earth surface land temperature spanning 1753 to 2011. Geoinfor. Geostat.: An Overview 1(1),

doi:http://dx.doi.org/10.4172/2327-4581.1000101.
Shang, H., Wei, W., Yuan, Y., Yu, S. and Zhang, T., 2011. Variations of temperature during last 350 years at Xinyuan recorded by tree-ring. J. Arid Land Resour. Environ. 25(9), 187–190 (in Chinese with English abstract).
Shao, X. et al., 2005. Reconstruction of precipitation variation from tree rings in recent 1000 years in Delingha, Qinghai. Sci. China Ser. D-Earth Sci. 48(7), 939–949.
Sheppard, P.R. et al., 2004. Annual precipitation since 515 BC reconstructed from living and fossil juniper growth of northeastern Qinghai Province, China. Clim. Dyn. 23(7–8), 869–881.
Shi, X. et al., 2010. May–June mean maximum temperature change during 1360–2005 as reconstructed by tree rings of Sabina Tibetica in Zaduo, Qinghai Province. Chin. Sci. Bull. 55(26), 3023–3029.
Song, H. and Liu, Y., 2011. PDSI variations at Kongtong Mountain, China, inferred from a 283-year *Pinus tabulaeformis* ring width chronology. J. Geophy. Res. 116, D22111, doi: 10.1029/2011jd016220.
Tian, Q. et al., 2007. Tree-ringbased drought reconstruction (a.d. 1855–2001) for the Qilian mountains, northwestern China. Tree-Ring Res. 63(1), 27–36.
Usoskin, I. and Mursula, K., 2003. Long-term solar cycle evolution: Review of recent developments. Solar Phys. 218(1–2), 319–343.
Wang, T., Ren, H. and Ma, K., 2005. Climatic signals in tree ring of *Picea schrenkiana* along an altitudinal gradient in the central Tianshan Mountains, northwestern China. Trees 19(6), 736–742.
Wigley, T.M.L., Briffa, K.R. and Jones, P.D., 1984. On the average value of correlated time series, with applications in dendroclimatology and hydrometeorology. J. Clim. Appl. Meteorol. 23, 201–213.
Wilson, R.J. and Luckman, B.H., 2003. Dendroclimatic reconstruction of maximum summer temperatures from upper treeline sites in Interior British Columbia, Canada. The Holocene 13(6), 851–861.
Yang, B., Qin, C., Bräuning, A., Burchardt, I. and Liu, J., 2011. Rainfall history for the Hexi Corridor in the arid northwest China during the past 620 years derived from tree rings. Int. J. Climatol. 31(8), 1166–1176.
Yu, S., Yuan, Y., He, Q., Li, J. and Wu, Z., 2007. Reconstruction of temperature series from AD 1468–2001 in the Jinghe, Xinjiang. J. Glaciol. Geocryol. 29(3), 374–379 (in Chinese with English abstract).
Yu, S. et al., 2008. Response of tree-ring to climate change and temperature reconstruction in west of Tianshan Mountains north slope. J. Desert Res. 28(5), 827–832 (in Chinese with English abstract).
Yuan, Y., Li, J. and Zhang, J., 2001. 348-year precipitation reconstruction from tree-rings for the north slope of the middle Tianshan mountains. Acta Meteorol. Sin. 15(1), 95–104.
Zhang, Y., Shao, X.M., Yin, Z.Y. and Wang, Y., 2014. Millennial minimum temperature variations in the Qilian Mountains, China: evidence from tree rings. Clim. Past 10(5), 1763–1778.
Zhu, H., Wang, L., Shao, X. and Fang, X., 2004. Tree ring-width response of *picea schrenkiana* to climate change. Acta Geogr. Sin. 59(6), 863–870 (in Chinese with English abstract).
Zhu, H. et al., 2008. Millennial temperature reconstruction based on tree-ring widths of Qilian juniper from Wulan, Qinghai Province, China. Chin. Sci. Bull. 53(24), 3914–3920.